*J. Fluid Mech.* (1995), *vol.* 303, *pp.* 83–102



# The unsteady motion of solid bodies in creeping flows

By J. FENG AND D. D. JOSEPH

Department of Aerospace Engineering and Mechanics and The Minnesota Supercomputer Institute, University of Minnesota, Minneapolis, MN 55455, USA

(Received 13 May 1994 and in revised form 18 July 1995)

In treating unsteady particle motions in creeping flows, a quasi-steady approximation is often used, which assumes that the particle's motion is so slow that it is composed of a series of steady states. In each of these states, the fluid is in a steady Stokes flow and the total force and torque on the particle are zero. This paper examines the validity of the quasi-steady method. For simple cases of sedimenting spheres, previous work has shown that neglecting the unsteady forces causes a cumulative error in the trajectory of the spheres. Here we will study the unsteady motion of solid bodies in several more-complex flows: the rotation of an ellipsoid in a simple shear flow, the sedimentation of two elliptic cylinders and four circular cylinders in a quiescent fluid and the motion of an elliptic cylinder in a Poiseuille flow in a two-dimensional channel. The motion of the fluid is obtained by direct numerical simulation and the motion of the particles is determined by solving their equations of motion with solid inertia taken into account. Solutions with the unsteady inertia of the fluid included or neglected are compared with the quasi-steady solutions. For some flows, the effects of the solid inertia and the unsteady inertia of the fluid are important quantitatively but not qualitatively. In other cases, the character of the particles' motion is changed. In particular, the unsteady effects tend to suppress the periodic oscillations generated by the quasi-steady approximation. Thus, the results of quasi-steady calculations are never uniformly valid and can be completely misleading. The conditions under which the unsteady effects at small Reynolds numbers are important are explored and the implications for modelling of suspension flows are addressed.

## 1. Introduction

The unsteady motion of solid particles at vanishing Reynolds numbers is a general problem and has been much studied since the classic paper of Stokes (1851). All previous works fall into two categories, each addressing one part of the problem. The first part is to formulate the hydrodynamic force on the particle as a function of the particles' configuration and motion. This enables one to write the correct equations of motion for the particles. The second part is to solve the equations of motion for the particles, and to predict interesting properties of the system, such as particle trajectories, concentration and configuration of an assemblage of particles and so forth. Obviously, attacking part two is contingent on a satisfactory solution of part one.

The first category contains the profound papers of Stokes (1851) and Basset (1888) and their generalizations to more complex flows. Stokes (1851) obtained the drag on a sphere that is oscillating along one of its diameters in a quiescent fluid. Basset (1888)

studied the flow caused by a sphere undergoing an arbitrary translational motion $U(t)$, and derived the following formula for the drag:

$$F = -6\pi\mu Ua - \tfrac{2}{3}\pi\rho a^3 \frac{dU}{dt} - 6\pi\mu a^2 \frac{1}{(\pi\nu)^{1/2}} \int_{-\infty}^{t} \frac{dU(\tau)}{d\tau} \frac{d\tau}{(t-\tau)^{1/2}}, \tag{1}$$

where $\rho$, $\mu$ and $\nu$ are the density, dynamic and kinematic viscosity of the fluid; $a$ is the radius of the sphere. The three terms on the right-hand side are the quasi-steady Stokes drag, the inertial drag due to added mass and the Basset force, respectively. Then the equation of motion for the particle under an external force $f(t)$ can be written as

$$\tfrac{4}{3}\pi a^3 \rho_s \frac{dU}{dt} = f(t) - 6\pi\mu Ua - \tfrac{2}{3}\pi\rho a^3 \frac{dU}{dt} - 6\pi\mu a^2 \frac{1}{(\pi\nu)^{1/2}} \int_{-\infty}^{t} \frac{dU(\tau)}{d\tau} \frac{d\tau}{(t-\tau)^{1/2}}, \tag{2}$$

where $\rho_s$ is the density of the solid sphere. This is also known as the Basset equation. Mazur & Bedeaux (1974) generalized equation (1) to the case where the fluid itself is in unsteady non-uniform motion. The convective inertia of the fluid flow is neglected. Maxey & Riley (1983) attacked the same problem but retained the convective inertia of the undisturbed flow. The equation of motion for a solid particle thus derived contains an additional term of inertial force due to the fluid flow. Also, the three terms on the right-hand side of (1) are each modified by a Faxén term proportional to $\nabla^2 \boldsymbol{u}$ which accounts for the effect of non-uniform shear in the fluid flow. This equation has been applied by Mei, Adrian & Hanratty (1991) to study the dispersion of fine particles in turbulence. Lawrence & Weinbaum (1986, 1988) have generalized equation (1) to a spheroid in axisymmetric motion. Their results show that for non-spherical particles the 'Basset term' is much more complicated than the Basset force in (1) and has different behaviour in time. Gavze (1990) presented a general formulation for the hydrodynamic force and torque that embraces arbitrary shape for the particle and non-uniform flow fields at infinity. Recently, Lovalenti & Brady (1993, 1995) calculated the Oseen correction to the unsteady drag on a sphere translating at small but finite Reynolds numbers. They found that inclusion of the Oseen inertia alters the long-term behaviour of the unsteady force. For a sphere accelerating from rest, the unsteady force decays as $t^{-2}$ instead of $t^{-1/2}$.

Analytical solutions to the second part of the problem are limited to spherical particles in a quiescent fluid, largely because of the complex forms of the history effect. Baggio (1907) solved the unsteady sedimentation of a sphere under the action of a constant gravity. Hinch (1975) gave the response of a spherical particle to an impulsive force that is a delta function in time. Arminski & Weinbaum (1979) inverted the Basset equation for an arbitrary external force $f(t)$ and discussed the behaviour of the sphere when $f(t)$ is of a 'top hat' and a single 'saw-tooth' form. A systematic exposition of these results is given in Kim & Karrila (1991).

An important goal of the analysis of particle motions is to evaluate the effects of the different unsteady forces at play. For example, if under certain conditions the force due to the unsteady history is small compared to the quasi-steady Stokes drag, we may ignore this term in modelling similar flows and the analysis can be greatly reduced. For a sedimenting sphere, it has been shown (Kim & Karrila 1991) that in a short time following the release of the particle, the acceleration of the particle, the added-mass force and the Basset force are equally important. Then the acceleration of the particle and the added-mass force die out quickly. The Basset force has a long-term influence that, if ignored, can cause large error in predicting the trajectory of the particle. Leichtberg *et al.* (1976) reported a thorough study of the sedimentation of three

identical spheres with their line of centres vertical. They used the method of multipole expansion to solve the manoeuvers of the particles in the presence of hydrodynamic interactions among them. By using the Basset force of a single sphere, they found that the error in trajectory grows with time as $t^{1/2}$ if the unsteady forces are neglected. The analyses of a single sphere and three spheres in sedimentation show that the unsteady forces, especially the Basset force, are of considerable influence on the motion of the particles. Ignoring the unsteady forces causes an error that accumulates in time, but the qualitative nature of the motion is not altered.

We have found no further studies in the second category of literature that deal with more complex flows involving, say, wall effects, particle–particle interactions, non-spherical particles and non-uniform flow fields. In fact, Leichtberg *et al.* (1976) could not formulate the correct Basset force for each sphere in the presence of other solid boundaries and had to use the Basset force for a single sphere. The success of this approach is explained by Lawrence & Weinbaum (1988), who showed that the Basset force for a spheroid is insensitive to its shape if the aspect ratio is not large. Their work also suggests that for more complex geometries, the unsteady force due to the history of the particle's acceleration cannot even be expressed in a form similar to the Basset integral. Because of the complexity of this effect, numerical analysis will have to take the place of traditional analysis in order to extend the line of research on unsteady forces and the motion of particles in creeping flows.

On the other hand, practical problems in engineering have long demanded treatment of far more complex processes such as slurry transportation and fluidization, and various theoretical models and prediction methods have been developed. It has been noted, however, that fundamental knowledge of the unsteady forces and the transient motion of particles is missing. Thus, these methods have invariably adopted the quasi-steady approach by completely ignoring the transient effects. A good example is Stokesian dynamics (Bossis & Brady 1984; Brady & Bossis 1988), a theoretical model for the motion of solid particles suspended in a creeping flow. At a given time, the velocities of all particles are determined by the external forces and torques on the suspension and the geometric configuration of the assemblage. The motion of each particle is then followed by moving it according to the velocity at the current time; the particle has instant acceleration and no equation of motion is needed. This is equivalent to setting the inertia of both the particles and the fluid to zero. In this sense, the Stokesian dynamics is a static, rather than dynamic, method. Despite the continued success of the theory (Brady & Bossis 1985; Durlofsky, Brady & Bossis 1987; Brady *et al.* 1988; Phillips, Brady & Bossis 1988*a*, *b*; Claeys & Brady 1993*a*–*c*; Chang & Powell 1993), the accuracy of using the quasi-steady scheme in tracking unsteady particle motions has never been examined. In the literature, the practice of completely ignoring the unsteady effects of inertia at low Reynolds numbers is overwhelming. The famous Jeffery orbit (Jeffery 1922) is obtained by setting the force and torque on the ellipsoid to zero, and so are the many generalizations of the Jeffery problem (e.g. Bretherton 1962; Chwang 1975; Yang & Leal 1984; Hsu 1985; Pittman & Kasiri 1992). Other works on particle motion in sedimentation and shear flows include Hocking (1964), Ganatos, Pfeffer & Weinbaum (1978), Kim (1985), Hassonjee, Pfeffer & Ganatos (1992) and Sugihara-Seki (1993). Among all these papers, only Ganatos *et al.* (1978) explicitly mentioned the error inherent in the quasi-steady method. Other authors may have either assumed the error to be trivial or have been too well aware that no better treatment is available.

This paper represents a preliminary attempt at questioning the validity of the quasi-steady approach. From previous studies of sedimentation we have learned that the

error in this approach is quantitatively appreciable but qualitatively insignificant. Here, several more complex cases will be examined by direct numerical simulations. As we will see in subsequent sections, the unsteady forces may completely change the characteristics of the particles' motion under certain circumstances.

## 2. Dimensional analysis

Generally, the motion of a solid particle in a fluid is governed by the following equations:

$$\left.\begin{aligned} &\rho(\partial \boldsymbol{u}/\partial t + \boldsymbol{u}\cdot\nabla\boldsymbol{u}) = -\nabla p + \mu\nabla^2\boldsymbol{u}, \\ &\nabla\cdot\boldsymbol{u} = 0, \\ &m\,\mathrm{d}V/\mathrm{d}t = \boldsymbol{F}, \end{aligned}\right\} \tag{3}$$

where $V$ is the velocity (or angular velocity) of the particle, $m$ its mass (or moment of inertia) and $\boldsymbol{F}$ the total force (or torque) on it. The characteristic length is the linear dimension of the particle $d$ and the characteristic velocity is a certain $U$. If one scales the time by $d/U$ and the force by $\mu Ud$, equation (3) can be made dimensionless:

$$\left.\begin{aligned} &Re\,(\partial \boldsymbol{u}/\partial t + \boldsymbol{u}\cdot\nabla\boldsymbol{u}) = -\nabla p + \nabla^2\boldsymbol{u}, \\ &\nabla\cdot\boldsymbol{u} = 0, \\ &\frac{m}{\rho d^3} Re\frac{\mathrm{d}V}{\mathrm{d}t} = \boldsymbol{F}, \end{aligned}\right\} \tag{4}$$

where the Reynolds number $Re = \rho Ud/\mu$. Now if one lets $Re \to 0$, the linearized equations are obtained:

$$\nabla p = \nabla^2\boldsymbol{u}, \quad \nabla\cdot\boldsymbol{u} = 0, \quad \boldsymbol{F} = 0. \tag{5}$$

This is the basis for the quasi-steady approach. The force-free and torque-free conditions imply that the particles adjust their velocities and angular velocities instantaneously.

The above derivation assumes that the unsteadiness of the motion is caused by the spatial variation of the undisturbed flow and is characterized by a time scale $T = d/U$. This is not universally true. In fact, the time scale $T$ depends on the nature of the flow and the properties of the solid body, and is thus unique to each flow situation. In this paper, we will study three problems: (i) the rotation of an ellipsoid in a simple shear flow (Jeffery 1922); (ii) the sedimentation of a few particles in a quiescent fluid (Kim 1985; Claeys & Brady 1993*a*) and (iii) the motion of an ellipse in a plane Poiseuille flow (Sugihara-Seki 1993). Quasi-steady solutions have been obtained by the authors listed above, and all three problems have periodic solutions. It is perhaps of interest to examine the characteristic time scale for each problem.

In problem (i), the rotation of the ellipsoid is a direct result of the shear flow and the angular velocity is proportional to the shear rate $\kappa$. This gives a characteristic time $T = \kappa^{-1}$. Then $\partial \boldsymbol{u}/\partial t$ and $\boldsymbol{u}\cdot\nabla\boldsymbol{u}$ are of the same order and equations (4) are justified. In problems (ii) and (iii), the unsteadiness is caused by hydrodynamic interactions among particles and particle–wall interactions, respectively. A common feature is the lateral manoeuver of the solid bodies across undisturbed streamlines; the time scale is determined by the period of this lateral oscillation. Let us assume that the lateral driving force on a particle is proportional to a characteristic velocity $U$:

$$f \sim \mu Ud.$$

Then the lateral acceleration of the particle is

$$f/m \sim \mu U d/m,$$

where $m$ is the sum of the mass and the virtual mass of the particle. The time needed for this particle to move a lateral distance of order $d$ is

$$T \sim \left(\frac{d}{f/m}\right)^{1/2} = \left(\frac{m}{\mu U}\right)^{1/2}.$$

This $T$ is preferred to $d/U$ as the characteristic time because $d/U$ describes the motion along the main flow of velocity $U$, while $T$ is able to describe the excursion of the particle in the direction perpendicular to the main flow, a feature that proves to be essential to the problems at hand. Now the unsteady terms can be scaled as

$$\frac{\partial \boldsymbol{u}}{\partial t} = \frac{U}{T}\frac{\partial \boldsymbol{u}^*}{\partial t^*} = \mathrm{U}\left(\frac{\mu U}{m}\right)^{1/2}\frac{\partial \boldsymbol{u}^*}{\partial t^*}.$$

And the dimensionless equations are (the asterisk has been omitted)

$$\left.\begin{aligned} &\left(\frac{\rho d^3}{m}\right)^{1/2} Re^{1/2}\frac{\partial \boldsymbol{u}}{\partial t} + Re\,\boldsymbol{u}\cdot\nabla\boldsymbol{u} = -\nabla p + \nabla^2\boldsymbol{u}, \\ &\nabla\cdot\boldsymbol{u} = 0, \\ &\left(\frac{m}{\rho d^3}\right)^{1/2} Re^{1/2}\frac{\mathrm{d}V}{\mathrm{d}t} = \boldsymbol{F}. \end{aligned}\right\} \tag{6}$$

Therefore, the unsteady terms are $Re^{-1/2}$ larger than the convective inertia for problems (ii) and (iii). If the Reynolds number approaches zero, eventually all terms on the left-hand sides of (6) are, of course, negligible. But for a particular Stokes approximation at a small but finite Reynolds number, it may be inappropriate to neglect both unsteady and convective inertial terms uniformly. The implications of the above analysis will become clear in the next section.

## 3. Numerical results

To illustrate the effects of the unsteady inertia, we take the three problems that have been solved by the quasi-steady method and re-solve them when (*a*) the inertia of the solid particle is added to equations (5) but the unsteady inertia of the fluid is not:

$$\left.\begin{aligned} &0 = -\nabla p + \mu\nabla^2\boldsymbol{u}, \\ &\nabla\cdot\boldsymbol{u} = 0, \\ &m\,\mathrm{d}V/\mathrm{d}t = \boldsymbol{F}, \end{aligned}\right\} \tag{7}$$

and (*b*) both inertial terms are present:

$$\left.\begin{aligned} &\rho\,\partial\boldsymbol{u}/\partial t = -\nabla p + \mu\nabla^2\boldsymbol{u}, \\ &\nabla\cdot\boldsymbol{u} = 0, \\ &m\frac{\mathrm{d}V}{\mathrm{d}t} = \boldsymbol{F}. \end{aligned}\right\} \tag{8}$$

This will allow us to evaluate the importance of the two transient terms. The convective inertia $\boldsymbol{u}\cdot\nabla\boldsymbol{u}$ is always neglected. An initial value problem based on (8) gives the behaviour of a temporal disturbance to (7). So in a sense, we are testing the stability of the quasi-steady solutions.

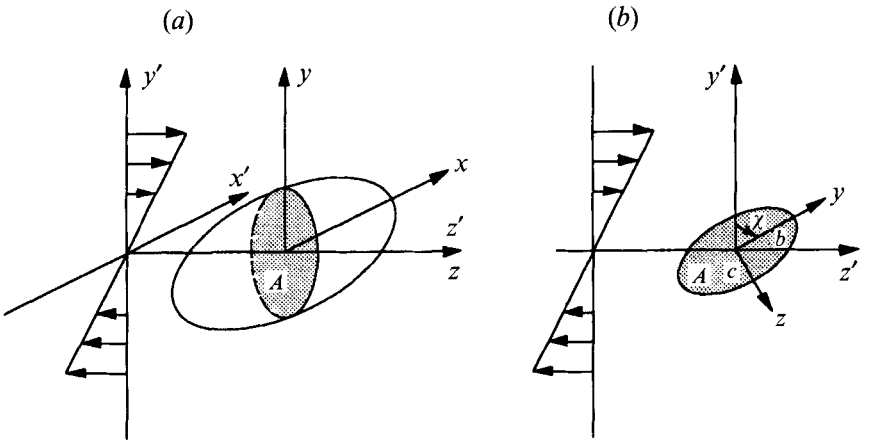


FIGURE 1. Jeffery's first solution. $(x', y', z')$ are coordinates fixed in space. The shear flow is $(u_o, v_o, w_o) = (0, 0, \kappa y')$, $\kappa$ being the shear rate. $(x, y, z)$ are coordinates fixed on the ellipsoid, and the equation of the ellipsoid is $x^2/a^2 + y^2/b^2 + z^2/c^2 = 1$. In this solution, $x$ is kept parallel to $x'$. (*a*) At $t = 0$, the angle $\chi = 0$; (*b*) the cross-section $A$ rotates in the $(y'z')$-plane with variable angular velocity.

The motion of solid particles is coupled with the steady or transient Stokes flow. The numerical solution is carried out using an explicit–implicit method that has been designed to simulate the fully nonlinear flow of fluid–particle systems. The Stokes flows are easily handled by a modified Navier–Stokes solver POLYFLOW. Details of the numerical schemes have been reported earlier (Hu, Joseph & Crochet 1992; Feng, Hu & Joseph 1994*a*, *b*; Feng, Huang & Joseph 1995) and will not be repeated here. The numerical algorithm only solves two-dimensional problems; if the original quasi-steady solution is in three dimensions, we will treat its two-dimensional counterpart.

The numerical data will be presented in dimensionless variables for generality. It is easy to see that after making equations (8) non-dimensional, the coefficients in front of $\partial \boldsymbol{u}/\partial t$ and $\mathrm{d}V/\mathrm{d}t$ are $\rho d^2/(\mu T)$ and $m/(\mu d T)$, respectively. If we use $T = d/U$, $U$ being a characteristic velocity, then the first parameter is a Reynolds number $Re = \rho U d/\mu$, and the second one depends on $Re$, the density ratio between the solid and the fluid $\rho_s/\rho$ and an aspect ratio of the solid body. Note that $Re$ can be absorbed into the time derivative. This implies that $Re$ will only affect the time scale of the problem through $T = \rho d^2/(\mu Re)$, and results that do not explicitly involve temporal evolution are valid for any $Re$. Therefore, the density ratio and geometry of the particle have to be specified for each set of data, whereas $Re$ need be given only for plots involving time. We remind the reader that $T = d/U$ is used for convenience in presenting the data and is not to be confused with the time scale established in §2.

### 3.1. *Rotation of an ellipsoid in a simple shear flow*

Jeffery (1992) studied the slow motion of a solid ellipsoid in a simple shear flow. Following the quasi-steady approach, he set the force and torque on the body to zero and obtained a system of differential equations describing the rotation of the ellipsoid. Analytical solutions were obtained for two special cases. The first is when one of the principal axes of the ellipsoid is kept parallel to the vorticity vector of the shear flow (figure 1). The ellipsoid rotates around this axis with variable angular velocity:

$$\dot{\chi} = \frac{\kappa}{b^2 + c^2}(b^2 \cos^2 \chi + c^2 \sin^2 \chi) \tag{9}$$

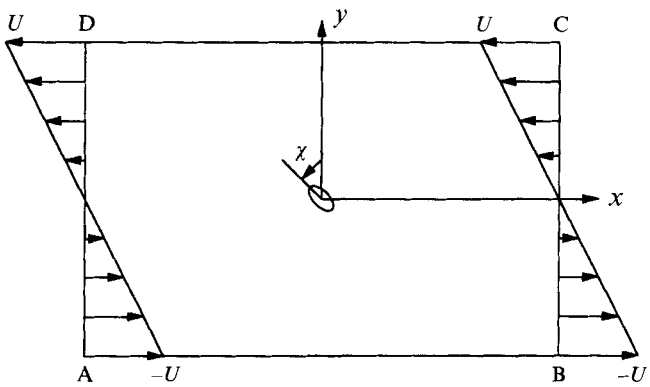


FIGURE 2. Computational domain for the rotation of an ellipse in a simple shear flow.

and the angle $\chi$ varies with time according to

$$\tan\chi = \frac{b}{c}\tan\frac{bc\kappa t}{b^2+c^2}. \tag{10}$$

Jeffery's second special case is for a spheroid ($b = c$). The body rotates around the axisymmetric axis $x$, while the axis itself precesses around the $x'$-axis, drawing a cone. The angle between the $x$- and $x'$-axes changes periodically during the revolution and is dependent on initial conditions. This dependency on initial conditions, or indeterminacy by itself, gives rise to the interesting problem of orbit evolution when a weak inertia perturbs the motion (Leal 1980).

Equations (9) and (10) do not depend on the semi-axis $a$, and the solution holds even if the ellipsoid is extended to infinity in the $x'$-direction to form an elliptic cylinder. So Jeffery's first solution applies to two dimensions and can be compared directly with our two-dimensional simulation. If $b = c$ in equation (9), we get $\dot{\chi} = \kappa/2$. It is a well-known result that a circular cylinder rotates with the local angular velocity of the fluid (Cox, Zia & Mason 1968). As a point of interest, one may note that (9) and (10) also describe the rotation of the spheroid projected onto the $(y', z')$-plane in Jeffery's second solution.

Our computational domain is shown in figure 2. The aspect ratio of the ellipse is 2:1; the lengths of the semi-axes are $b$ and $c = b/2$. The density of the solid matches that of the fluid. The inlet and outlet boundaries (BC and DA) are each $20b$ away from the centre of the ellipse, and undisturbed linear velocity profiles are imposed on them, with a shear rate $\kappa$. The two other boundaries AB and CD are each $10b$ away from the centre of the ellipse, and they are taken to be undisturbed streamlines. Since the Jeffery solution is for an unbounded domain, we have conducted numerical tests of the effects of the four boundaries. Results show that the domain described above is large enough.

The ellipse is initially at $\chi = 0$, and an initial angular velocity $\dot{\chi} = 0.8\kappa$ is applied to be consistent with equation (9). The undisturbed linear velocity field is used as the initial condition. The rotation obtained with and without the unsteady inertia of the fluid is compared with equations (9) and (10) in figure 3. The three numbered curves are very close in figure 3(*a*). The solid inertia causes a slight deviation from the Jeffery solution (curve 2). If the fluid transient is included (curve 3), this deviation becomes larger but still small; the ellipse turns a little ahead of the other two cases. The differences $\chi_3 - \chi_1$ and $\chi_2 - \chi_1$ are also depicted in figure 3(*a*). They tend to grow in time, though it is not clear whether the error will eventually go to infinity. Immediately

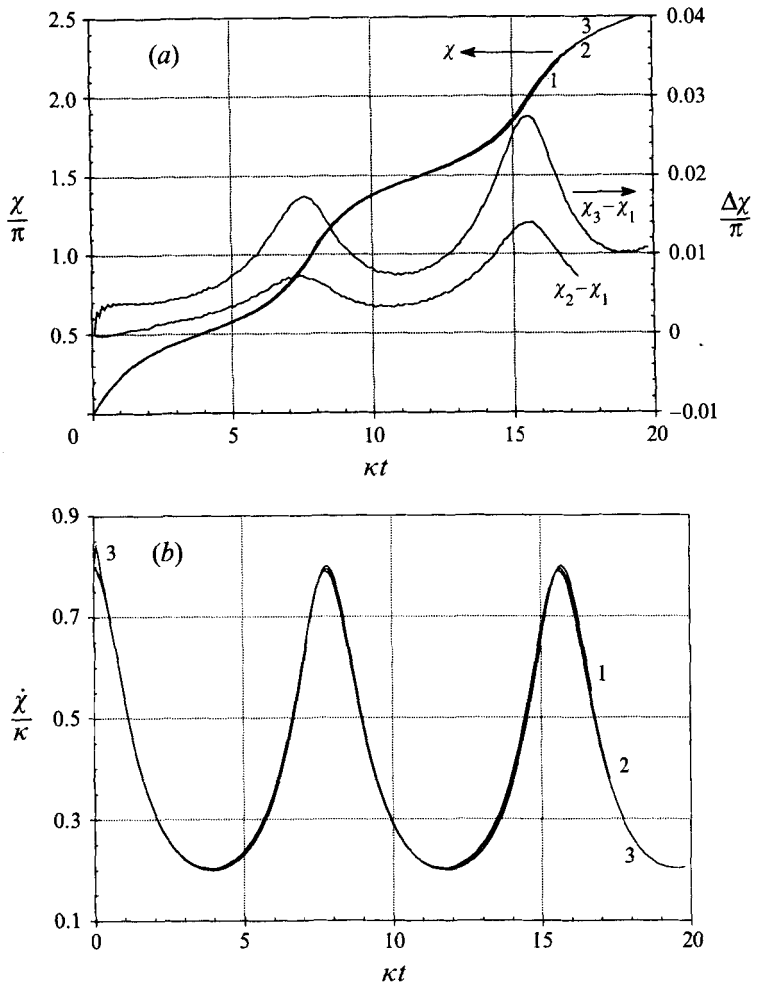


FIGURE 3. The rotation of an ellipse in a simple shear flow. The Reynolds number $Re = \rho b^2\kappa/\mu = 0.25$. Curve 1 is the quasi-steady Jeffery solution; curves 2 and 3 are our numerical solutions, without and with the transient term $\partial \boldsymbol{u}/\partial t$, respectively. (*a*) Variation of the angle $\chi$; (*b*) variation of the angular velocity $\dot{\chi}$. The abscissa is the dimensionless time.

after release the ellipse acquires an angular velocity remarkably larger than the theoretical value (figure 3*b*). But later, this difference disappears and all three curves stay close. The oscillation in $\dot{\chi}$ has a slightly smaller amplitude when the solid and fluid inertia are included in turn.

We conclude from figure 3 that the moment of inertia of the ellipse has a weak effect on its rotation. The influence of the unsteady fluid inertia adds to that of the solid inertia, but the difference it makes is still small in the time our computation covers. The error does tend to grow as time goes on. We emphasize that reducing *Re* will only expand the time scale of the flow, and will not reduce the discrepancy among the three curves.

### 3.2. *Sedimentation in a quiescent fluid*

Kim (1985) and Claeys & Brady (1993*a*) have analysed the motion of two identical spheroids settling side by side in an infinite expanse of fluid. Kim used the method of reflections and Claeys & Brady's approach is an extension of Stokesian dynamics to

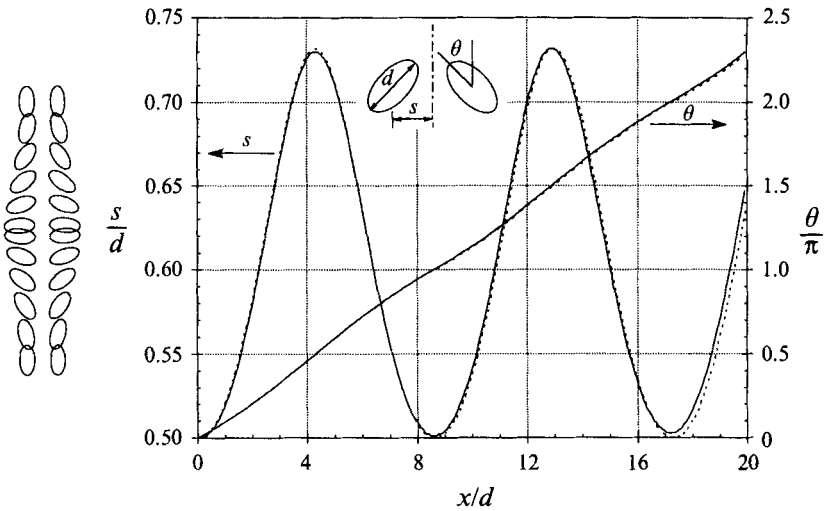


FIGURE 4. Sedimentation of two ellipses in the absence of fluid inertia $\partial \boldsymbol{u}/\partial t$: $\rho_s/\rho = 1.003$; $s$ is half of the centre-to-centre separation between ellipses; $\theta$ is the angle of rotation and $x$ is the vertical distance of fall. Solid lines represent the solution when solid inertia is considered, and the sketch on the left shows snapshots of the ellipses in the first 'cycle'. Dashed lines represent the quasi-steady solution.

non-spherical particles. Both studies used the quasi-steady approximation by neglecting the inertia of the spheroids and that of the fluid, and their results agree. Initially, the major axes of both spheroids are parallel to gravity. If the initial separation is small, the particles rotate and drift away from each other while falling till their major axes are horizontal. Then they approach each other and return to the initial configuration. The cycle is repeated and a periodic motion is obtained. If the initial separation is larger than a critical value, the spheroids will drift farther and farther apart, and no periodic solution exists.

We compute the sedimentation of two ellipses of aspect ratio 2:1. Because our numerical program works only in two dimensions, the results cannot be directly compared to Kim (1985) or Claeys & Brady (1993*a*). The major axis is of length $d$; the initial centre-to-centre distance is $d$. This separation gives a periodic solution in Kim (1985) and Claeys & Brady (1993*a*). The computational domain is $10d$ wide and $25d$ high, with the particles' centres $10d$ above the bottom boundary, and the domain moves with the particles (Feng *et al.* 1994*a*). Zero velocity is imposed on all boundaries except the 'outlet' above the particles, where zero-force condition is used. The density of the ellipse $\rho_s$ is larger than that of the fluid $\rho$.

First, we obtain a quasi-steady solution for our two-dimensional sedimentation following Kim (1985). The solution is periodic, of course, but the amplitude of oscillation is much smaller than that given by Kim (1985) and Claeys & Brady (1993*a*). This is probably because the motion is two-dimensional here. The walls that bound the computational domain may also be responsible.

Next we take into account the solid inertia but leave out the $\partial \boldsymbol{u}/\partial t$ term in the governing equations for the fluid and release the ellipses from rest. In the time our computation covers, the two particles remain symmetric. The trajectory and rotation of one ellipse are compared with the quasi-steady solution in figure 4. The solid inertia causes a small deviation from the perfectly periodic solution; the difference grows with time in much the same way as in Jeffery's solution (figure 3). Numerical tests show that

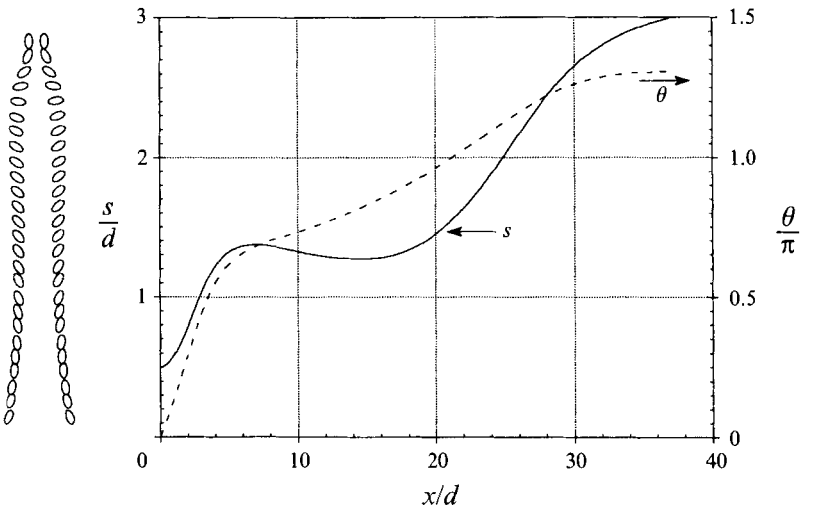


FIGURE 5. Sedimentation of two ellipses in the presence of fluid inertia $\partial \boldsymbol{u}/\partial t$: $\rho_s/\rho = 1.003$.

the discrepancy becomes more pronounced if $\rho_s/\rho$ is increased. Since the ellipses are released from rest, the initial transient could contribute to the difference in trajectory. To check this effect, we did simulations in which the ellipses were released with initial velocity and angular velocity that match those of the quasi-steady solution. The trajectory differs little from the solid curve in figure 4, and the initial transient can be dismissed.

We have re-computed the problem with the $\partial \boldsymbol{u}/\partial t$ term retained. The results, shown in figure 5, are vastly different from the curves in figure 4. After the ellipses turn to horizontal ($\theta = \pi/2$), they continue to move apart for a while. Then they start to move inward. But long before they could return to the initial separation, they move outward again. This drifting apart is never reversed. At the end of the computation, the ellipses are close to the vertical boundaries and wall effects may have come into play. But one can easily imagine that the particles would drift apart indefinitely in an unbounded fluid. This picture bears some resemblance to the experiment of Jayaweera & Mason (1965) on two circular cylinders settling side by side.

Next, we turn to another sedimentation problem in which interactions among particles give rise to periodic solutions in the limit of quasi-steadiness. Hocking (1964) and Durlofsky *et al.* (1987) have studied the falling of four identical spheres initially located at the corners of a square of side $S_0$; the square is in the vertical plane of gravity. The top two spheres will 'penetrate' the bottom two and re-form the square. The cycle repeats indefinitely. We have carried out two-dimensional simulations on four settling circular cylinders released from rest. For this example, we did not calculate the quasi-steady solution. The solid inertia is always retained and the trajectories of particles are obtained by solving the Newton equation of motion. Two cases, with and without the transient inertia of the fluid, are computed. The diameter of the cylinders is $d$ and the initial separation $S_0 = 1.5d$, which is equivalent to $L = 3$ in figure 6 of Durlofsky *et al.* (1987).

Figure 6 shows the results when $\partial \boldsymbol{u}/\partial t$ is neglected. The square is transformed into a rectangle at the end of the first 'cycle'. The horizontal separation between spheres is still $1.5d$, but the vertical separation has become $1.64d$. After the second inversion, the rectangle has grown to $1.54d \times 1.8d$. This deviation from a periodic solution evidently results from the inertia of the solid particles and is expected to grow as in figure 4.

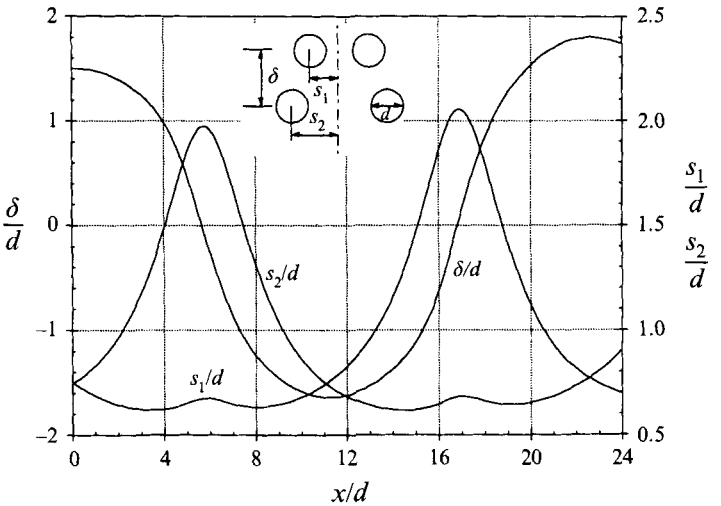


FIGURE 6. Sedimentation of four particles in the absence of fluid inertia $\partial \boldsymbol{u}/\partial t$: $\rho_s/\rho = 1.003$; $x$ is the vertical distance of fall defined for the mid-point between the upper and lower pairs.

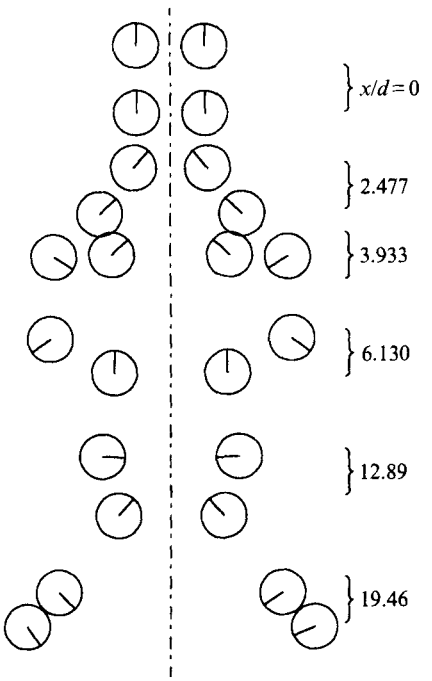


FIGURE 7. Snapshots of the four particles taken at different times during the sedimentation: $\rho_s/\rho = 1.003$. The unsteady inertia of the fluid $\partial \boldsymbol{u}/\partial t$ is included. The last two shots have been moved upward for a better view.

When the unsteady inertia of the fluid is included, the sedimentation is strongly aperiodic (figure 7). At the beginning of the fall, the two top particles get closer and the bottom two get farther apart as in figure 6. Then the top particles seem to follow the bottom ones and move outwards. By the time all four lie on a horizontal line, the two particles on the left are close to each other and so are the two on the right. But the two pairs are rather far apart (figure 7, $x/d = 3.933$). Unlike the quasi-steady case, all

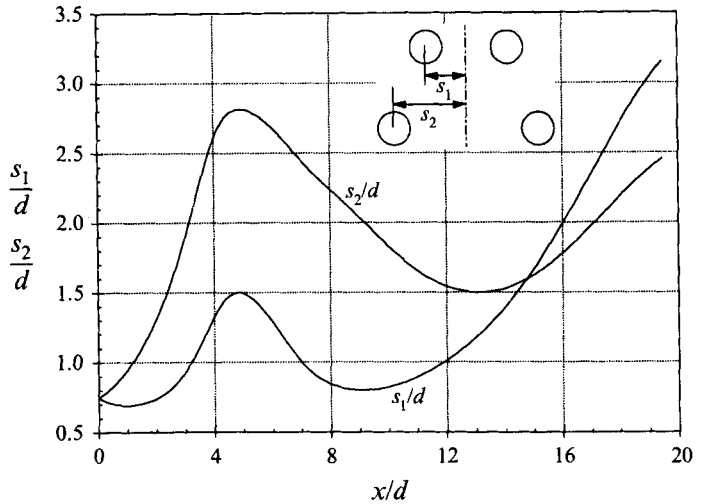


FIGURE 8. Sedimentation of four particles when fluid inertia $\partial \boldsymbol{u}/\partial t$ is included: $\rho_s/\rho = 1.003$.

particles are still moving outwards at this time (see figure 8). This is seen as an effect of the fluid's inertia. After that, the two particles in the middle fall faster and take the lead (figure 7, $x/d = 6.13$). But the lateral distance between the two outside particles remains large and the square is never restored (figure 8). From then on, the motion of two particles on either side is somewhat similar to that of a doublet governed by the fully nonlinear Navier–Stokes equations (Hu *et al.* 1992; Feng *et al.* 1994*a*); the particle on top tends to follow and approach that one at bottom.

In summary, the solid inertia causes a small yet cumulative deviation from the periodic quasi-steady solutions. The inclusion of the unsteady inertia of the fluid changes the characteristic of the motion in the two examples considered: it causes a loss of periodicity in the quasi-steady solution. When $Re \to 0$, the curves in figures 5 and 8 will not change; the time scale will blow up. Thus, the quasi-steady trajectory will be close to the true trajectory for a finite time, which is longer for smaller $Re$. But the approximation is never uniformly valid. Also note that as $Re$ approaches zero, the period of the quasi-steady solution goes to infinity; the periodicity is spurious and can never be observed experimentally. As suggested by the dimensional analysis in §2, the $Re^{1/2}$ terms can be important and neglecting them can lead to unstable results.

### 3.3. *Motion of an ellipse in a Poiseuille flow*

Sugihara-Seki (1993) published a numerical simulation of the motion of a neutrally buoyant ellipse in a Poiseuille flow in the limit of $Re = 0$. The steady Stokes problem is solved for a prescribed position and orientation of the ellipse and the velocity and the angular velocity of the ellipse are computed from the condition of vanishing force and torque. The neighbouring quasi-steady states are then connected to form the trajectory of the ellipse. The geometry of the problem is shown in figure 9. Depending on the initial configuration and geometry of the ellipse, three types of periodic motion can be obtained: (i) continuous rotation in one direction (tumbling) between a wall and the centreline of the channel; (ii) oscillation with the long axis swinging about $\theta = 90°$ and its centre swinging across the centreline; (iii) oscillation with the long axis in a small-amplitude swing about $\theta = 0°$. Type (iii) has an important degenerate case in which the oscillation has zero amplitude and the ellipse slides steadily at $y_c = y^*$, $\theta = 0°$. For all three types of motion, the amplitude of oscillation and the average

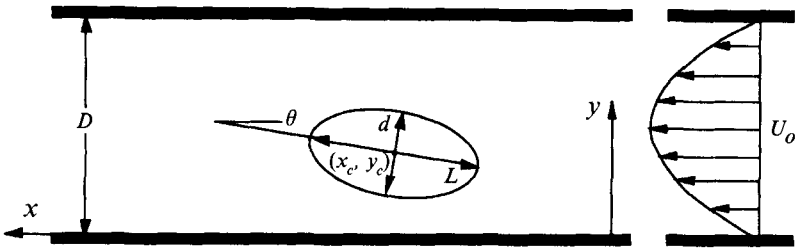


FIGURE 9. The ellipse and the Poiseuille flow in a two-dimensional channel. $U_o$ is the maximum velocity of the undisturbed flow and $D$ is the channel width. The ellipse's centre is at $(x_c, y_c)$ and the major and minor axes are $d$ and $L$; its shape is specified by $\alpha = d/L$ and its size by $\beta = dL/D^2$.

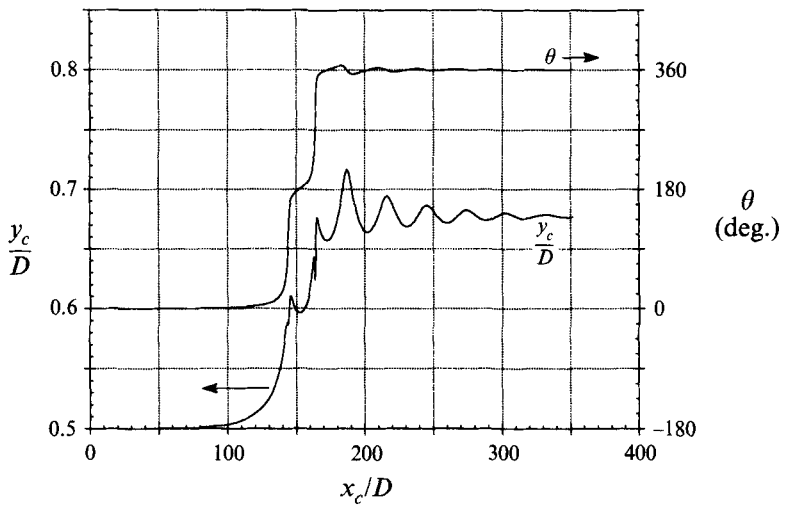


FIGURE 10. The motion of the small ellipse, $\alpha = 0.5$, $\beta = 0.25$. The inertia of the ellipse is taken into account but the inertia of the fluid is not. The initial configuration is $(y_o/D, \theta_o) = (0.5, 0°)$.

position of the ellipse depend on the initial configurations $(y_o/D, \theta_o)$. For motions (i) and (iii), the average position of the ellipse's centre also depends on its shape and size (given by $\alpha = d/L$ and $\beta = dL/D^2$); type (i) is always between type (iii) and the centreline. As $\beta$ increases to a critical value $\beta^*$, $y^*$ shifts to the centreline, and the tumbling motion of type (i) is 'squeezed out' and never occurs. Thus, for large ellipses there are only two types of oscillation; both are around the centreline, with $\theta$ swinging around 0° and 90°, respectively.

In our simulations, we adopt the same $\alpha, \beta$ values as in Sugihara-Seki: $\alpha = 0.5$ and $\beta = 0.25$ as the small ellipse and $\alpha = 0.5$ and $\beta = 0.4$ as the large ellipse. For $\alpha = 0.5$, the critical value $\beta^* = 0.334$. The ellipse is neutrally buoyant in the fluid. Again, two cases are studied, using equations (7) and (8), respectively.

If the unsteady fluid inertia is neglected, our results show that the only stable motion for the small ellipse is the steady motion that Sugihara-Seki (1993) obtained as a degenerate case of type (iii). We have tested four different initial configurations: $(y_0/D, \theta_o) = (0.8, 0°)$, which would give an oscillation of type (iii) in the quasi-steady limit; $(y_o/D, \theta_o) = (0.6, 0°)$, which would give the tumbling motion (i); $(y_o/D, \theta_o) = (0.5, 89.4°)$, which would give the oscillation of type (ii) and $(y_o/D, \theta_o) = (0.5, 0°)$, which is an unstable equilibrium position that would lead to either type (i) or type (ii) motion. In all four cases, the ellipse eventually assumes a steady motion with $(y_c/D, \theta) = (0.6775, 0°)$; this $y_c$ value agrees almost exactly with $y^*$ of Sugihara-Seki. Figure 10

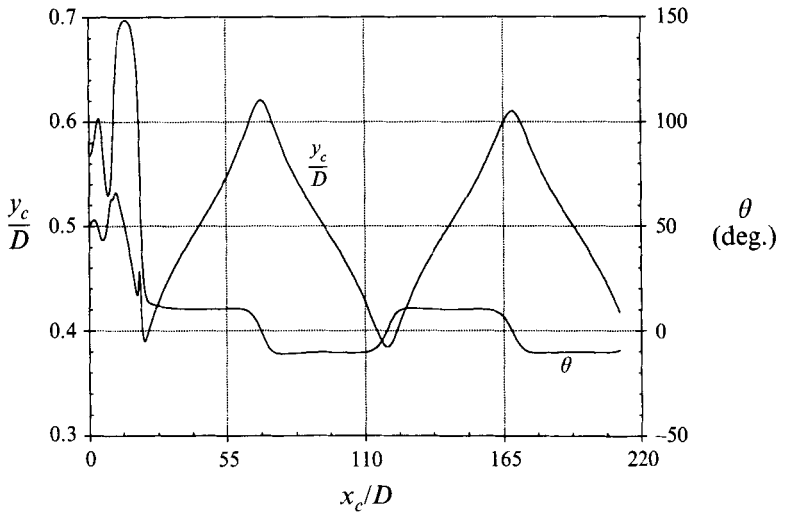


FIGURE 11. The motion of the large ellipse, $\alpha = 0.5$, $\beta = 0.4$. The inertia of the ellipse is taken into account but the inertia of the fluid is not. The initial configuration is $(y_o/D, \theta_o) = (0.5, 84°)$.

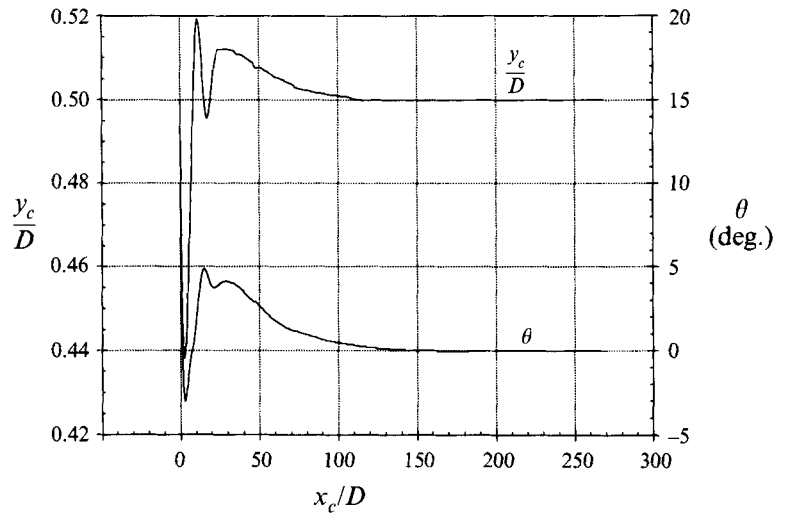


FIGURE 12. Motion of the large particle when the unsteady inertia of the fluid $\partial \boldsymbol{u}/\partial t$ is included. The initial configuration is $(y_o/D, \theta_o) = (0.5, 9°)$.

shows the motion starting from $(y_o/D, \theta) = (0.5, 0°)$. Immediately after release, the ellipse slides along the centreline. Then it starts to drift upward at $x_c/D \approx 60$. The velocity gradient makes the ellipse tumble twice as it goes up. Finally a steady solution is reached. Transients starting from other initial configurations also involve tumbling and sidewise drift.

The large ellipse is released on the centreline of the channel at four initial tilt angles: $\theta_o = 0°, 9°, 36°$ and $84°$. According to Sugihara-Seki (1993), the first angle $\theta_o = 0°$ leads to a stable steady solution $(y_c/D, \theta) = (0.5, 0°)$. The second tilt angles $\theta_o = 9°$ gives the type (iii) oscillation, and the other two give type (ii) oscillations of different amplitudes. In our numerical simulations, the steady motion at the centreline is obtained, but the other three cases all evolve into the same type (iii) oscillation. Figure 11 gives the

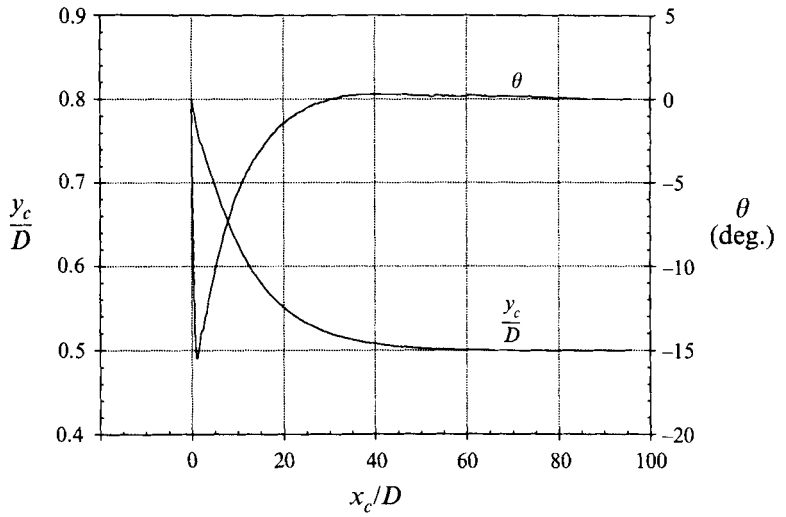


FIGURE 13. Motion of the small particle when the unsteady inertia of the fluid $\partial \boldsymbol{u}/\partial t$ is included. The initial configuration is $(y_o/D, \theta_o) = (0.8, 0°)$.

trajectory starting with $\theta_o = 84°$. At the beginning of the motion, the ellipse does attempt to oscillate around $\theta = 90°$. The amplitude grows and the oscillation transforms into one around $\theta = 0°$. In Sugihara-Seki (1993), the amplitude of type (iii) oscillations is determined by the initial configuration. Here, the same periodic solution is attained for all three non-zero initial angles tested. It would be interesting to see the transition between the steady symmetric motion and the oscillation. But this is not related to our purpose in this report.

If the unsteady inertia $\partial \boldsymbol{u}/\partial t$ is included, the only stable solution, for both particle sizes and all initial configurations we have tested, is a steady motion along the centreline: $(y_c/D, \theta) = (0.5, 0°)$. Figures 12 and 13 shows two typical cases.

We were surprised that the tumbling motion of type (i) was unreachable in all the simulations discussed above. Not only is this mode of motion an exact solution to the quasi-steady Stokes flow (Chwang 1975), it has also been observed in experiments (Karnis, Goldsmith & Mason 1963, 1966). Then we realized that our small ellipse ($\alpha = 0.5$, $\beta = 0.25$) was still too large for tumbling to occur. Numerical tests were carried out for a smaller ellipse with $\alpha = 0.5$, $\beta = 0.005$ ($L/D = 0.1$). Results without and with the unsteady inertia of the fluid are shown in figures 14 and 15. The motion in figure 14 agrees qualitatively with Chwang's theory. Variations in the angular velocity and the longitudinal velocity of the ellipse are almost periodic; there is no lateral migration. Moreover, the angular velocity is roughly the same as the Jeffery spin if the local shear rate is used in equations (9) and (10). The only effect of the parabolic velocity profile is the variable translational velocity. Chwang's theory was constructed for a spheroid in a general paraboloidal flow, yet the rotation is the same as that of an ellipse in a planar Poiseuille flow. One wonders if the formula for angular velocity is valid for a general ellipsoid, as Jeffery's first solution is. The inclusion of solid inertia has the same effect on the particle's motion as in figure 3. When the unsteady fluid inertia is added (figure 15), the tumbling of the ellipse still exists. There is also a preferred position of equilibrium. An ellipse released at $(u_o/D, \theta_o) = (0.6, 0°)$ tumbles while drifting slowly toward the centre (curves *a* and *b*). Another ellipse initially at $(y_o/D, \theta_o) = (0.51, 0°)$ only drifts very slightly outward (curves *c* and *d*). The angular velocity for the latter

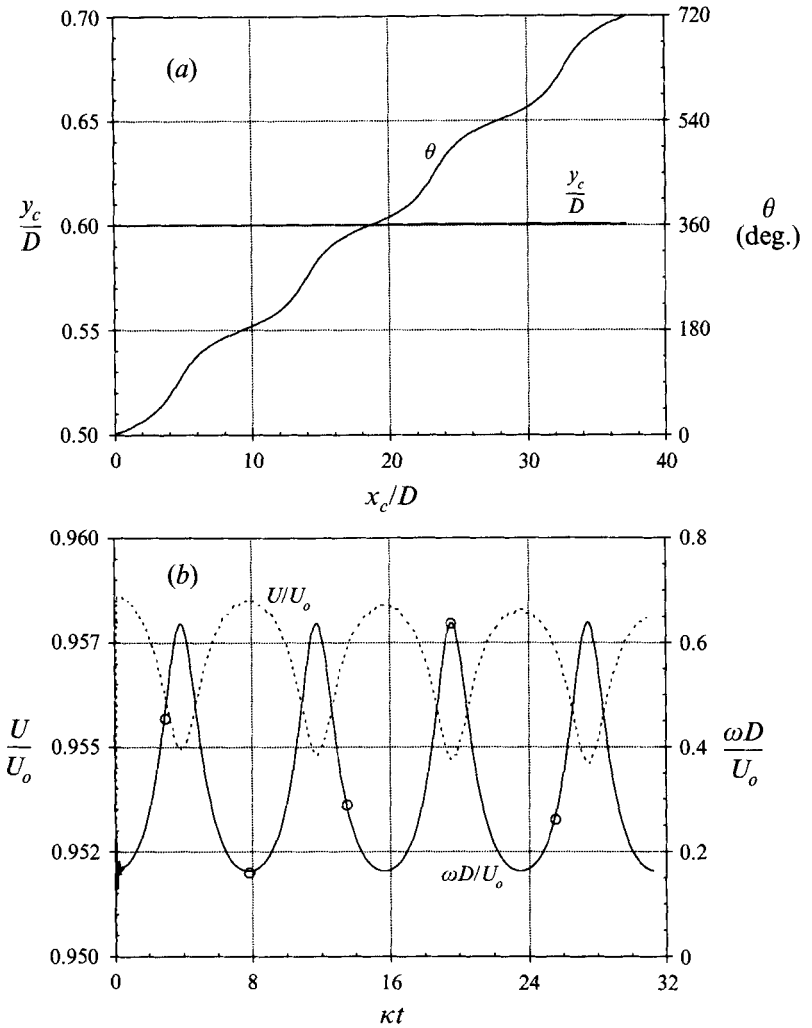


FIGURE 14. The motion of a small ellipse ($\alpha = 0.5, \beta = 0.005$) in a Poiseuille flow. The unsteady inertia of the fluid is neglected. Initially $(y_c/D, \theta) = (0.6, 0°)$. (*a*) Trajectory and rotation; (*b*) translational and angular velocities. The data points represent Jeffery's first solution (equation (9)). Time is scaled by the local shear rate $\kappa$, and the Reynolds number is $Re = \rho U_o L^2/(4\mu D) = 0.25$.

case is much smaller because the local shear rate is small. We did not carry the two runs further because of high computing cost. But it is clear from figure 15 that the transient inertia of the fluid defines an equilibrium position between the centreline and the wall. This is consistent with the experimental observations of Karnis *et al.* (1966). The remarkable differences among figures 10, 11 and 14 suggest the extreme importance of wall effects. In fact, the characteristic time scale in figures 14 and 15 is determined by the shear of the flow, like in the Jeffery's solution, rather than the particle–wall interaction (cf. §2). The motions examined here are examples to show the importance of the unsteady inertia in creeping flows. There may be other patterns of motion for larger and smaller ellipses.

From the above results, we note that the solid inertia and the unsteady fluid inertia tend to suppress periodic motions and favour steady motions. This seems to be natural if the very definition of inertia is considered as related to Newton's first law of motion.

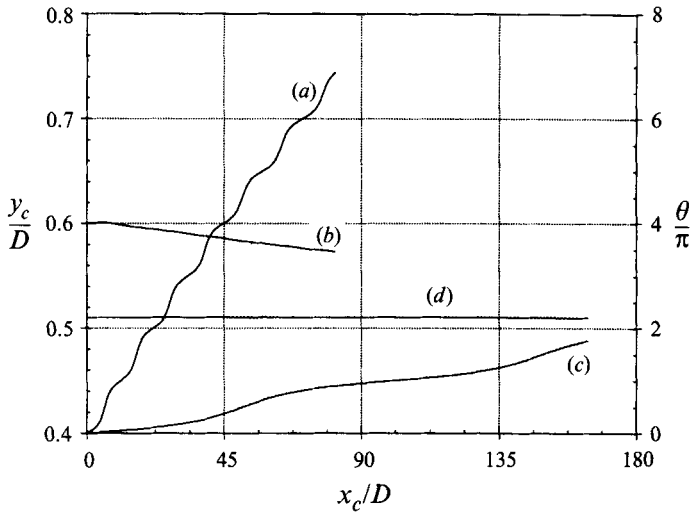


FIGURE 15. The motion of a small ellipse ($\alpha = 0.05$, $\beta = 0.005$) in a Poiseuille flow. The unsteady inertia of the fluid $\partial \boldsymbol{u}/\partial t$ is included. Curves (*a*) and (*b*) are the lateral position and angle of rotation for an ellipse initially at $(y_c/D, \theta) = (0.6, 0°)$; curves (*c*) and (*d*) are the same for an ellipse initially at $(y_c/D, \theta) = (0.51, 0°)$.

Sugihara-Seki's result is kinematic in essence. The periodicity arises merely as a result of geometric symmetry. Our results show that for relatively large ellipses, these periodic solutions are not stable to temporal disturbances. In experiments, the periodic solutions of Sugihara-Seki (1993) can never be observed and the physical picture they give is completely misleading.

If the entire fluid inertia $\partial \boldsymbol{u}/\partial t + \boldsymbol{u} \cdot \nabla \boldsymbol{u}$ is considered, a large ellipse assumes a steady motion slightly off the centreline with a small tilt angle (Feng *et al.* 1995). Thus, the quasi-steady solution, the solution with solid inertia only, the solution with solid inertia and unsteady fluid inertia and the solution with the nonlinear fluid inertia all look qualitatively different. Yet, the governing equations (3), (5), (7) and (8) approximate one another for small Reynolds numbers. The key is to realize that these equations represent entirely different physical processes at non-vanishing Reynolds numbers, and they approach the same limit when $Re$ goes to zero. So as $Re \to 0$, the period of Sugihara-Seki's oscillatory solutions goes to infinity, and the position of the particle approaches the centreline. The common limit then appears to be a steady solution with the ellipse lying symmetrically on the centreline. Adding the two $Re^{1/2}$ terms to equations (5) gives a much better approximation to the nonlinear exact solution.

## 4. Discussion

The numerical simulations reported here point to the fact that under certain circumstances, the inertia of the solid particles and the unsteady inertia of the fluid can change the characteristics of the particles' motion in creeping flows. Under other conditions, however, these two factors only cause quantitatively significant errors and have little effect on the pattern of the motion. A natural question is: what flow situations are more susceptible to the influence of unsteady inertia? A complete answer to this question is not available. From the results we have obtained, the following factors seem relevant.

(*a*) The unsteadiness of the quasi-steady Stokes motion. If the temporal variation of the basic solution is mild, adding the transient terms will not change the nature of the flow; the resulting motion will still be mildly unsteady. For instance, in the sedimentation of a sphere or a few spheres in a vertical line (Leichtberg *et al.* 1976), the time dependency is only reflected by the increase in the falling velocity and the change in interparticle separations; the basic configuration is not changing in time. Then the unsteady forces cause an accumulative error in the trajectory, but the nature of the motion is not affected. Another example is the cross-stream migration of a small sphere in a planar Poiseuille flow (Ho & Leal 1974). The quasi-steady motion is time-dependent only because the sphere experiences stronger or weaker wall effects and shear at different locations. The quasi-steady method gives qualitatively the same prediction as the direct simulation of the Navier–Stokes equations (Feng *et al.* 1994*b*).

(*b*) The nature of periodicity in the basic solution. Even if the motion is highly unsteady, such as a periodic oscillation, it can be strongly resistant to transient effects if the time-dependency is 'robust'. Jeffery's first solution is periodic. But the rotation is a direct result of the shear flow and is very robust. On the other hand, the periodic settling of two ellipses and four circles and the various oscillatory motions of Sugihara-Seki are determined by particle–particle and particle–wall interactions. The periodic nature is dependent on the symmetry of the configurations, not directly on the undisturbed flow. As a result, the motions are not as robust as Jeffery's first solution. This robustness seems to correlate well with the relative magnitude of the $\partial \boldsymbol{u}/\partial t$ term discussed in §2.

(*c*) Wall effects. Leichtberg *et al.* (1976) mentioned that solid walls can strongly affect unsteady forces. In our simulations, the tumbling motion (Sugihara-Seki's type i) cannot be realized if the particle is too large, or equivalently, the walls are too close. This gives new evidence that walls tend to enhance the unsteady inertial effects and make quasi-steady solutions unstable to temporal disturbances imposed by the transient terms.

In an infinite domain, a steady flow past a two-dimensional object has no solution (Stokes' paradox) while an unsteady flow does. This seems to suggest a fundamental difference between steady and unsteady Stokes flows. It is not clear how this argument relates to our numerical results obtained in bounded domains. Besides, it appears unlikely that the drastic effects of unsteady forces exist only in two dimensions.

All the flows considered in §3, even when the convective inertia is included, can be easily solved by direct simulations of the Navier–Stokes equations. For complex systems, such as a suspension under shear, simulations can be done only for the linearized problem. Then an immediate question arises about the unsteady effects in these systems. How do the transient terms affect the collective properties of a suspension? Will methods like Stokesian dynamics suffer serious errors in certain flow situations because of their quasi-steady nature? These are important issues that need to be thoroughly investigated.

This work was supported by the NSF, Fluid, Particulate and Hydraulic Systems, the US Army, Mathematics and AHPCRC, the DOE, Department of Basic Energy Sciences and the Schlumberger Foundation, J.F. acknowledges support from the Graduate School of the University of Minnesota through a Doctoral Dissertation Fellowship.

## REFERENCES


ARMINSKI, L. & WEINBAUM, S. 1979 Effect of waveform and duration of impulse on the solution to the Basset–Langevin equation. *Phys. Fluids* **22**, 404–411.

BAGGIO, T. 1907 Integrazione dell'equazione funzionale che regge la caduta di una sfera in un liquido viscoso. *Atti. Accad. naz. Lincei* **16**, 730–737.

BASSET, A. B. 1888 On the motion of a sphere in a viscous liquid. *Phil. Trans. R. Soc. Lond.* A **179**, 43–63. (Also in *A Treatise on Hydrodynamics*, Chap. 22. Dover, 1961.)

BOSSIS, G. & BRADY, J. F. 1984 Dynamic simulation of sheared suspensions. *J. Chem. Phys.* **80**, 5141–5154.

BRADY, J. F. & BOSSIS, G. 1985 The rheology of concentrated suspensions of spheres in simple shear flow by numerical simulation. *J. Fluid Mech.* **155**, 105–129.

BRADY, J. F. & BOSSIS, G. 1988 Stokesian dynamics. *Ann. Rev. Fluid Mech.* **20**, 111–157.

BRADY, J. F., PHILLIPS, R. J., LESTER, J. C. & BOSSIS, G. 1988 Dynamic simulation of hydrodynamically interacting suspensions. *J. Fluid Mech.* **195**, 257–280.

BRETHERTON, F. P. 1962 The motion of rigid particles in a shear flow at low Reynolds number. *J. Fluid Mech.* **14**, 284–304.

CHANG, C. & POWELL, R. L. 1993 Dynamic simulation of bimodal suspensions of hydrodynamically interacting spherical particles. *J. Fluid Mech.* **253**, 1–25.

CHWANG, A. T. 1975 Hydromechanics of low-Reynolds-number flow. Part 3. Motion of a spheroidal particle in quadratic flows. *J. Fluid Mech.* **72**, 17–34.

CLAEYS, I. L. & BRADY, J. F. 1993*a* Suspensions of prolate spheroids in Stokes flow. Part 1. Dynamics of a finite number of particles in an unbounded fluid. *J. Fluid Mech.* **251**, 411–442.

CLAEYS, I. L. & BRADY, J. F. 1993*b* Suspensions of prolate spheroids in Stokes flow. Part 2. Statistically homogeneous dispersions. *J. Fluid Mech.* **251**, 443–477.

CLAEYS, I. L. & BRADY, J. F. 1993*c* Suspensions of prolate spheroids in Stokes flow. Part 3. Hydrodynamic transport properties of crystalline dispersions. *J. Fluid Mech.* **251**, 479–500.

COX, R. G., ZIA, I. Y. & MASON, S. G. 1968 Particle motions in sheared suspensions. XXV. Streamlines around cylinders and spheres. *J. Colloid Interface Sci.* **27**, 7–18.

DURLOFSKY, L., BRADY, J. F. & BOSSIS, G. 1987 Dynamic simulation of hydrodynamically interacting particles. *J. Fluid Mech.* **180**, 21–49.

FENG, J., HU, H. H. & JOSEPH, D. D. 1994*a* Direct simulation of initial value problems for the motion of solid bodies in a Newtonian fluid. Part 1. Sedimentation. *J. Fluid Mech.* **261**, 95–134.

FENG, J., HU, H. H. & JOSEPH, D. D. 1994*b* Direct simulation of initial value problems for the motion of solid bodies in a Newtonian fluid. Part 2. Couette and Poiseuille flows. *J. Fluid Mech.* **277**, 271–301.

FENG, J., HUANG, P. Y. & JOSEPH, D. D. 1995 Dynamic simulation of the motion of capsules in pipelines. *J. Fluid Mech.* **286**, 201–227.

GANATOS, P., PFEFFER, R. & WEINBAUM, S. 1978 A numerical-solution technique for three-dimensional Stokes flows, with application to the motion of strongly interacting spheres in a plane. *J. Fluid Mech.* **84**, 79–111.

GAVZE, E. 1990 The accelerated motion of rigid bodies in non-steady Stokes flow. *Intl J. Multiphase Flow* **16**, 153–166.

HASSONJEE, Q., PFEFFER, R. & GANATOS, P. 1992 Behavior of multiple spheres in shear and Poiseuille flow fields at low Reynolds number. *Intl J. Multiphase Flow* **18**, 353–370.

HINCH, E. J. 1975 Application of the Langevin equation to fluid suspensions. *J. Fluid Mech.* **72**, 499–511.

HO, B. P. & LEAL, L. G. 1974 Inertial migration of rigid spheres in two-dimensional unidirectional flows. *J. Fluid Mech.* **65**, 365–400.

HOCKING, L. M. 1964 The behavior of clusters of spheres falling in a viscous fluid. *J. Fluid Mech.* **20**, 129–139.

HSU, R. 1985 Hydrodynamic interaction of an arbitrary particle with a planar-wall at low Reynolds numbers. PhD thesis, City College of New York.

HU, H. H., JOSEPH, D. D. & CROCHET, M. J. 1992 Direct simulation of fluid particle motions. *Theoret. Comput. Fluid Dyn.* **3**, 285–306.

JAYAWEERA, K. O. L. F. & MASON, B. J. 1965 The behavior of freely falling cylinders and cones in a viscous fluid. *J. Fluid Mech.* **22**, 709–720.

JEFFERY, G. B. 1922 The motion of ellipsoidal particles immersed in a viscous fluid. *Proc. R. Soc. Lond.* A **102**, 161–179.

KARNIS, A., GOLDSMITH, H. L. & MASON, S. G. 1963 Axial migration of particles in Poiseuille flow. *Nature* **200**, 159–160.

KARNIS, A., GOLDSMITH, H. L. & MASON, S. G. 1966 The flow of suspensions through tubes. V. Inertial effects. *Can. J. Chem. Engng* **44**, 181–193.

KIM, S. 1985 Sedimentation of two arbitrarily oriented spheroids in a viscous fluid. *Intl J. Multiphase Flow* **11**, 699–712.

KIM, S. & KARRILA, S. J. 1991 *Microhydrodynamics: Principles and Selected Applications.* Butterworth-Heinemann.

LAWRENCE, C. J. & WEINBAUM, S. 1986 The force on an axisymmetric body in linearized, time-dependent motion: a new memory term. *J. Fluid Mech.* **171**, 209–218.

LAWRENCE, C. J. & WEINBAUM, S. 1988 The unsteady force on a body at low Reynolds number, the axisymmetric motion of a spheroid. *J. Fluid Mech.* **189**, 463–489.

LEAL, L. G. 1980 Particle motion in a viscous fluid. *Ann. Rev. Fluid Mech.* **12**, 435–476.

LEICHTBERG, S., WEINBAUM, S., PFEFFER, R. & GLUCKMAN, M. J. 1976 A study of unsteady forces at low Reynolds number: a strong interaction theory for the coaxial settling of three or more sphere. *Phil. Trans. R. Soc. Lond.* A **282**, 585–613.

LOVALENTI, P. M. & BRADY, J. F. 1993 The hydrodynamic force on a rigid particle undergoing arbitrary time-dependent motion at small Reynolds number. *J. Fluid Mech.* **256**, 561–605.

LOVALENTI, P. M. & BRADY, J. F. 1995 The temporal behavior of the hydrodynamic force on a body in response to an abrupt change in velocity at small but finite Reynolds number. *J. Fluid Mech.* **293**, 35–46.

MAXEY, M. R. & RILEY, J. J. 1983 Equation of motion for a small rigid sphere in a nonuniform flow. *Phys. Fluids* **26**, 883–889.

MAZUR, P. & BEDEAUX, D. 1974 A generalization of Faxén's theorem to nonsteady motion of a sphere through an incompressible fluid in arbitrary flow. *Physica* **76**, 235–246.

MEI, R., ADRIAN, R. J. & HANRATTY, T. J. 1991 Particle dispersion in isotropic turbulence under Stokes drag and Basset force with gravitational settling. *J. Fluid Mech.* **225**, 481–495.

PHILLIPS, R. J., BRADY, J. F. & BOSSIS, G. 1988*a* Hydrodynamic transport properties of hard-sphere dispersions. I. Suspensions of freely mobile particles. *Phys. Fluids* **31**, 3462–3472.

PHILLIPS, R. J., BRADY, J. F. & BOSSIS, G. 1988*b* Hydrodynamic transport properties of hard-sphere dispersions. II. Porous media. *Phys. Fluids* **31**, 3473–3479.

PITTMAN, J. F. T. & KASIRI, N. 1992 Motion of rigid rod-like particles suspended in non-homogeneous flow fields. *Intl J. Multiphase Flow* **18**, 1077–1091.

STOKES, G. G. 1851 On the effect of the internal friction of fluids on the motion of pendulums. *Trans. Camb. Phil. Soc.* **9** (II), 8–106.

SUGIHARA-SEKI, M. 1993 The motion of an elliptical cylinder in channel flow at low Reynolds numbers. *J. Fluid Mech.* **257**, 575–596.

YANG, S.-M. & LEAL, L. G. 1984 Particle motion in Stokes flow near a plane fluid-fluid interface. Part 2. Linear shear and axisymmetric straining. *J. Fluid Mech.* **149**, 275–304.